Optimal Placement of Thyristor Controlled Series Compensators for Sensitive Nodes in Transmission System Using Voltage Power Sensitivity Index

Saurabh Ratra, Pradeep Singh, and Rajive Tiwari
Department of Electrical Engineering, Malaviya National Institute of Technology, Jaipur, India
Email: {saurabhratra, psn121988, rajivetiwari72}@gmail.com

***Abstract*—This paper proposes a novel Voltage Power Sensitivity Index (VPSI) to find sensitive nodes for optimal placement of TCSCs. The proposed index is used to rank the buses according to their voltage sensitivity. Taguchi Method (TM) is used to find size of TCSCs to improve voltage stability margin and voltage profile of the system and to cope up the problem of line congestion. The proposed methodology has been tested on IEEE 14-bus test system to substantiate its applicability.**

***Index Terms*—voltage magnitude, TCSC, sensitivity index, L-index, MVA limits**

I. Introduction

With increasing size of power system along with Technical, Economical and Environmental (TEE) constraints, the probable menace of voltage instability is prominent in the power system networks [1]. Many incidents related to voltage collapse have been reported worldwide [1]-[4].

The problems related to voltage instability is related to inadequate reactive power supply, heavy loading on transmission lines, power shipping across long distances. To avoid voltage collapse either load is to be curtailed or Flexible Alternating Current Transmission System (FACTS) controller is to be placed at optimal locations. Introducing FACTS devices at appropriate locations are the most pragmatic way to enhance voltage profile, which in turn improves Voltage Stability Margin (VSM) [5].

The suitable locations for placing FACTS devices for improving VSM are voltage- sensitive nodes [6], [7]. In literature many researchers have reported methods or techniques to forecast voltage collapse and to identify weak nodes. Conventionally PV and QV curves were used to identify critical buses. These curves are generated through large data of repetitive load-flow solutions which require large time and also found to be computationally inefficient. Various other methods are also reported in literatures i.e. L-index [8], modal analysis [9], Line Collapse Proximity Index (LCPI) [10] etc. to identify weak buses or lines.

Manuscript received August 22, 2016; revised December 12, 2016.

This paper proposes Voltage Power Sensitivity Index *(VPSI)* to find voltage sensitive nodes of power systems. Proposed index identifies the voltage sensitive nodes of power system. Higher value of proposed index for a bus indicates higher voltage-sensitivity of the bus. Then the FACTS Controller (series or shunt) is placed on the weakest bus.

The remaining paper is organized as follows: Section II present indices for identifying critical lines/buses. Section III presents Thyristor Controlled Series Compensation (TCSC) Modelling. In Section IV, proposed index is presented. In Section V problem formulation is discussed. Simulation results and discussions on IEEE 14-bus test system are presented to authenticate the feasibility in Section VI. Conclusion is presented in Section VII.

II. Indices for Identifying Critical Lines or Buses

Voltage stability indices identify the weakest node or the critical line denoted to that bus. Some of the well-known indices are briefly described in this section.

A. PV Curve

PV curves shows variation in voltage of receiving end voltage with change in active power loading. Loading margin of a bus is distance of the current operating point in the PV curve with nose point. A system has as many P-V curves as there are lines in the system. Lower loading margin corresponding to a bus represents weak bus of the system. These curves are generally cast off to identify the loading margin of the power system [2].

B. QV Curve

QV curve helps the operator to know the maximum reactive power which can be added to the bus before reaching to its critical limit. The distance of MVAr from operating point till end of QV curve is known as reactive power margin [2].

C. L-Index

The utmost weakest bus of the system is determined through L- index [8] for a particular loading condition.

doi: 10.18178/ijoee.4.4.194-198

The value of L-index varies between zero to one from no load to a maximum loading point. If the assessed value tending towards 1.0, it shows that the bus or node is critically stressed and voltage collapse may occur.

D. Modal Analysis

In this analysis, smallest Eigen value and its related eigenvectors are calculated. The Eigen value near to zero specifies that the system is on the verge of PoC and probability of instability is very high [9]. This proximity of PoC can be forecast through the assessment of positive Eigen value. The weakest bus of the system can be determined by computing the Eigen vector for different buses in the system.

III. TCSC Modelling

The main advantage of using TCSC is voltage support. The TCSC, in combination with series capacitors, produce reactive power which increases with line loading, thereby alleviating voltage instability. The impedance model uses power flow concept to exemplify TCSC [11], [12]. The reactance is evaluated through power flow, then its firing angle is determined by αTCSC. The TCSC reactance X_{TCSC1} is known as [13]:

$$X_{TCSC1} = -X_C + C_1\{2(\pi-\alpha)+\sin 2(\pi-\alpha)\} - C_2\cos^2(\pi-\alpha)\{\varpi(\pi-\alpha)-\tan(\pi-\alpha)\} \qquad (1)$$

where,

$$C_1 = \frac{X_C + X_{LC}}{\pi}$$

$$X_{LC} = \frac{X_C X_L}{X_C - X_L} \qquad (2)$$

$$\varpi = \left(\frac{X_C}{X_L}\right)^{\frac{1}{2}}$$

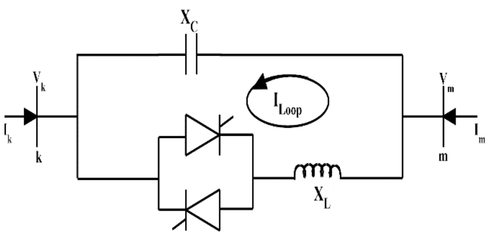

Figure 1. Equivalent TCSC model

Thyristor controlled series compensator model is shown in Fig. 1, and the Y_{Bus} matrix for Fig. 1 can be given as [14]:

$$\begin{pmatrix} I_k \\ I_m \end{pmatrix} = \begin{pmatrix} jB_{kk} & jB_{km} \\ jB_{nk} & jB_{nm} \end{pmatrix}\begin{pmatrix} V_k \\ V_m \end{pmatrix} \qquad (3)$$

For inductive mode,

$$\left.\begin{aligned} B_{kk} = B_{km} &= \frac{-1}{X_{TCSC}} \\ B_{km} = B_{mk} &= \frac{1}{X_{TCSC}} \end{aligned}\right\} \qquad (4)$$

Whereas in capacitive mode, the signs are inverted. The power equations have active and reactive power at bus *k* are:

$$P_k = V_k V_m B_{km}\sin(\delta_k - \delta_m) \qquad (5)$$

$$Q_k = -V_k^2 B_{kk} - V_k V_m B_{km}\, cos(\delta_k - \delta_m) \qquad (6)$$

where

$$B_{kk} = -B_{km} = B_{TCSC} \qquad (7)$$

At bus *m* subscripts *k* and *m* are swapped in eq.(4) and (5), whereas when TCSC control active power flow via bus *k* to bus *m*, the pair of linearized power flow equations are given as [15], [16]:

$$\begin{bmatrix} \Delta P_k \\ \Delta P_m \\ \Delta Q_k \\ \Delta Q_m \\ \Delta P_{km}^{\alpha_{TCSC}} \end{bmatrix} = \begin{bmatrix} \frac{\partial P_k}{\partial \delta_k} & \frac{\partial P_k}{\partial \delta_m} & \frac{\partial P_k}{\partial V_k}V_k & \frac{\partial P_k}{\partial V_m}V_m & \frac{\partial P_k}{\partial \alpha} \\ \frac{\partial P_m}{\partial \delta_k} & \frac{\partial P_m}{\partial \delta_m} & \frac{\partial P_m}{\partial V_k}V_k & \frac{\partial P_m}{\partial V_m}V_m & \frac{\partial P_m}{\partial \alpha} \\ \frac{\partial Q_k}{\partial \delta_k} & \frac{\partial Q_k}{\partial \delta_m} & \frac{\partial Q_k}{\partial V_k}V_k & \frac{\partial Q_k}{\partial V_m}V_m & \frac{\partial Q_k}{\partial \alpha} \\ \frac{\partial Q_m}{\partial \delta_k} & \frac{\partial Q_m}{\partial \delta_m} & \frac{\partial Q_m}{\partial V_k}V_k & \frac{\partial Q_m}{\partial V_m}V_m & \frac{\partial Q_m}{\partial \alpha} \\ \frac{\partial P_{km}^{\alpha_{TCSC}}}{\partial \delta_k} & \frac{\partial P_{km}^{\alpha_{TCSC}}}{\partial \delta_k} & \frac{\partial P_{km}^{\alpha_{TCSC}}}{\partial \delta_k} & \frac{\partial P_{km}^{\alpha_{TCSC}}}{\partial \delta_k} & \frac{\partial P_{km}^{\alpha_{TCSC}}}{\partial \delta_k} \end{bmatrix} \begin{bmatrix} \Delta\delta_k \\ \Delta\delta_m \\ \frac{\Delta V_k}{V_k} \\ \frac{\Delta V_m}{V_m} \\ \Delta\alpha_{TCSC} \end{bmatrix} \qquad (8)$$

where

$\Delta P_{km}^{\alpha_{TCSC}} = P_{km}^{reg} - P_{km}^{\alpha_{TCSC,cal}}$: is active power flow dissimilarity for TCSC module.

$\Delta\alpha_{TCSC} = \alpha_{TCSC}^{i+1} - \alpha_{TCSC}^{i}$: incremental change at i^{th} iteration of TCSC firing angle.

$P_{km}^{\alpha_{TCSC,cal}}$: calculated power between kth and m^{th} nodes.

IV. Proposed Index

A new perception of sensitivity is introduced in this paper. Bus voltage for different loading condition is measured and then their average value is calculated. Deviation of average voltage from base case is defined as Voltage Power Sensitivity Index (*VPSI*). Nodes with higher deviations are more sensitive nodes.

Mathematically, the proposed voltage power sensitivity index (*VPSI*) can be represented by

$$\Delta V_i = V_i^{Base} - \frac{1}{N_L}\sum_{l=1}^{N_L} V_i^l \qquad \forall\ i \in TN_B \qquad (9)$$

where *i* represents number of buses, *l* represents loading state and TN_B represents total number of buses.

The index for every bus in the system is near to 0, the system is stable.

As the sensitivity of any bus is higher, it means the active power flow equation has greater impact on voltage profile of the system. Similarly, all buses are arranged in descending order of *VPSI*.

$$VPSI = \begin{bmatrix} VPSI_1 \\ VPSI_2 \\ VPSI_3 \\ . \\ . \\ . \\ VPSI_i \end{bmatrix} \qquad (10)$$

i = number of buses

V. Problem Formulation

Optimal locations of TCSCs are most voltage sensitive buses which are selected on the basis of proposed index. Sizing of TCSCs is selected using Taguchi's method [17]. The problem formulation for identification of weak buses and computing the size of TCSC includes the following steps:

Step 1: For the base case system (considering without FACTS controller) the voltage profile is evaluated for each bus and is referred as voltage profile at base case.

Step 2: From calculations, Proposed *VPSI* is evaluate for each bus.

Step 3: Rank the critical buses in descending order based on *VPSI*.

Step 4: Finally using Taguchi Method (TM) optimal size of TCSC is identified.

The mathematical formulation is represented in following way:

Find X_{TCSC} to Minimize *VPSI*,

Subject to following constraints

$$P_i = V_i \sum_{j=1}^{nb} V_j [G_{ij}\cos(\delta_i - \delta_j) + B_{ij}\sin(\delta_i - \delta_j)] = P_{Gi} - P_{Di} \tag{11}$$

$$Q_i = \sum_{j=1}^{nb} V_j [G_{ij}\cos(\delta_i - \delta_j) - B_{ij}\sin(\delta_i - \delta_j)] = Q_{Gi} - Q_{Di} \tag{12}$$

$$j = 1, 2, \ldots nb$$

$$V_{Gi}^{\min} \le V_{Gi} \le V_{Gi}^{\max} \tag{13}$$

where *nb* is the number of buses, P_{Gi} and Q_{Gi} are active and reactive power at generation end of i^{th} bus. P_{Di} and Q_{Di} are active and reactive power at generation end of ith bus. G_{ij} and B_{ij} are conductance and Susceptance connected between lines *ij*. $V_{Gi}^{\min}$ and $V_{Gi}^{\max}$ are lower and higher limits of voltage magnitude and generator end.

VI. Results and Discussions

The proposed technique is tested on standard IEEE 14-bus test system as shown in Fig. 2, in which the critical nodes and location of TCSCs are mentioned. Initially the weak buses are identified using proposed method and ranked on the basis of severity. The ranking is verified on the basis of existing standard P-V curve and L-index. Two most critical buses are chosen for placement of TCSC's and their sizing is computed using Taguchi method so as to improve VSM and line congestion. The results of simulation with TCSC's are also compared without TCSC's in the following section.

A. PV Curves

PV curve are plotted for each bus by raising real power load of the bus. Fig. 3 illustrates the PV curves for IEEE 14-bus test system. As seen from Fig. 2, with an increase in loading factor λ, there is a dip in voltage profile of all buses. However, the rate of voltage decrement at bus 14 is quite high. Thus PV curve indicates that bus 14 is the most critical bus.

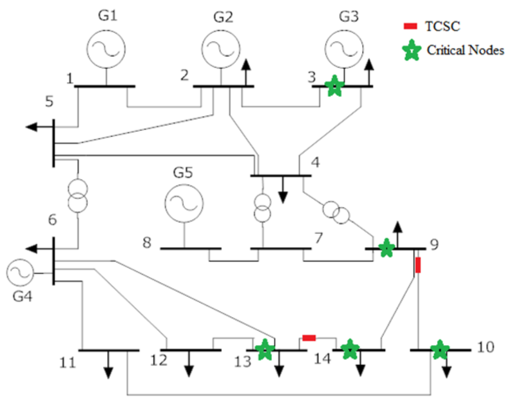

Figure 2. An IEEE 14-bus equivalent diagram

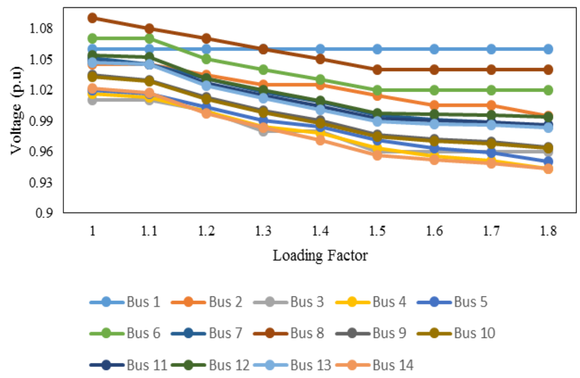

Figure 3. PV curves for all buses of IEEE 14-bus

B. L-Index

In Fig. 4, L-index for each PV bus is plotted at different loading factors (λ). L-index of bus 14 is observed to be higher than other buses. As λ is increasing, the bus 14 is increasing rapidly towards PoC. Hence from voltage stability stand point, bus 14 is the most critical for the system. Other critical buses are also identified on the basis of Fig. 4.

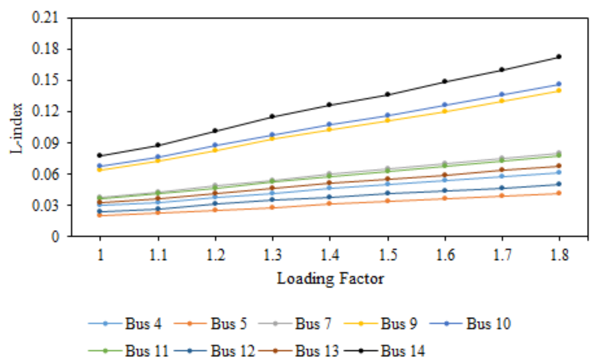

Figure 4. L-indices for all load buses of IEEE 14-bus system.

C. VPSI Index

Proposed *VPSI* is evaluated for each bus and results are shown in Table I. The maximum value of *VPSI* is reported at bus 14. This reveals that the bus is the most critical for the system. Buses are ranked on the basis of proposed method which is shown in Table II. The same ranking was obtained on the basis L-index. It verifies the proposed method.

TABLE I. VPSI FOR ALL BUSES OF IEEE 14-BUS SYSTEM

Bus No.	*VPSI*
1	0
2	0.006
3	0.037
4	0.0325
5	0.0281
6	0.021
7	0.0283
8	0.01
9	0.0429
10	0.0444
11	0.0351
12	0.0331
13	0.0373
14	0.0543

TABLE II. SENSITIVITY RANKING FOR CRITICAL BUSES

Rank	Bus No.	*VPSI*
1	14	0.0543
2	10	0.0444
3	9	0.0429
4	13	0.0373
5	3	0.037

D. Placement of TCSC Controller

The voltage sensitivity of each bus is evaluated on the basis of proposed sensitivity index. Buses are ranked according proposed sensitive index. Bus no 14 and 10 are two most sensitive buses as shown in Table II. Two TCSCs are chosen to be placed in line 13-14 and in line 10-11. Sizing of TCSCs are computed on the basis of Taguchi's method. TM provides two sets of reactance according to larger the better and smaller the better approach. These two cases are shown in Table III.

It is seen from Table III, that if case 1 is opted for placement of TCSC's, then the *VPSI* is higher which shows poor voltage profile and decreased voltage stability margin. Therefore, no fruitful results are obtained through Case 1. However if case 2 is selected, the *VPSI* is lower which shows that if TCSC's reactance are selected according to case 2, systems voltage profile and voltage stability margin will improve. Therefore, case 2 is an optimal choice for placement of TCSC's.

TABLE III. CONDITIONAL CASES FOR TCSC'S PLACEMENT

Condition	$TCSC_1$ (X)	$TCSC_2$ (X)	*VPSI*	Remarks
Case 1	0.34802	0.19207	0.0543	Worst
Case 2	-j0.06960	-j0.03841	0.0494	Best

Effect of placement of TCSCs on *VPSI* before and after TCSC placement is shown in Fig. 5. It is clearly visible from Fig. 5 that the use of TCSC at the two weakest buses reduces the sensitivity index. The reduction in sensitivity index implies the improved voltage stability margin. The results are supported on the basis of L-index as shown in Fig. 6.

The effect of TCSC's on voltage profile is also observed under different loading conditions. The voltage profile of most critical bus i.e. bus 14 is shown in Fig. 7. It shows that the use of TCSC controllers improve voltage profile of most of the buses in the system.

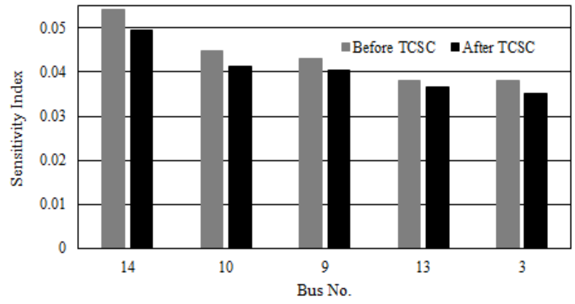

Figure 5. Sensitivity index before and after placement of TCSC.

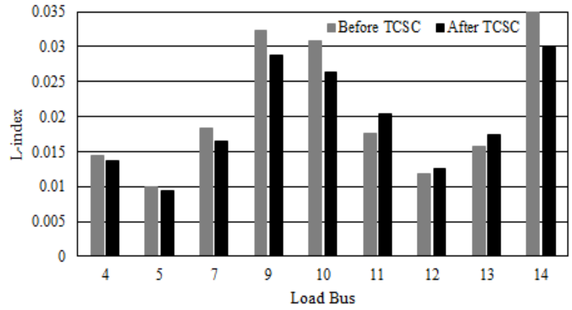

Figure 6. L-index before and after placement of TCSC

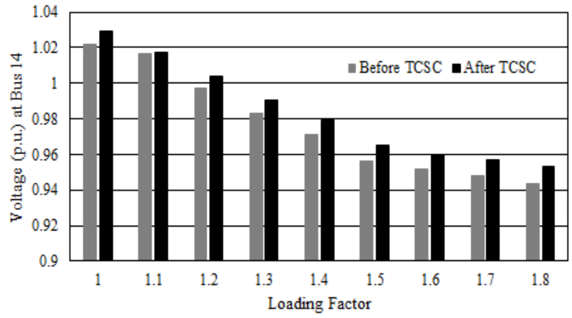

Figure 7. Voltage profile at bus 14 before and after TCSC.

For a particular loading factor it is observed that power flow in the lines 1-5 and 4-5 are above the line limits. Placement of TCSCs assists in alleviating the congestion of lines. Fig. 8 shows that after placement of TCSCs, power flow in all the branches are under their MVA limits and system is far away from congestion.

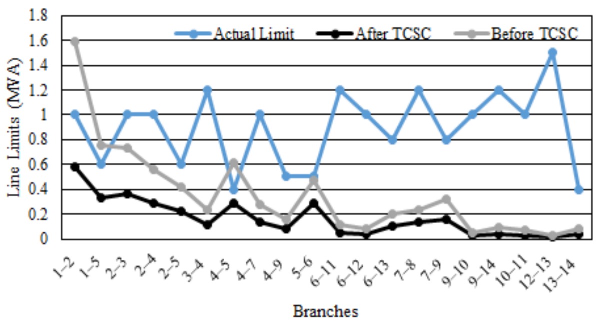

Figure 8. MVA line limits before and after placement of TCSC.

VII. CONCLUSION

In this paper, a novel Voltage Power Sensitivity Index (*VPSI*) is proposed to identify critical nodes for optimal placement of TCSC's. Placement of TCSCs with proper sizing resulted in improved voltage stability margin, better voltage profile, and reduced overloading of lines. Effect of TCSC's on other performance parameters of power systems can also be investigated.

REFERENCES

[1] D. Rimorov, I. Kamwa, and G. Joós, "Quasi-Steady-State approach for analysis of frequency oscillations and damping controller design," *IEEE Transactions on Power Systems*, vol. 31, no. 4, pp. 3212-3220, 2016.

[2] P. Kundur, *et al.*, "Definition and classification of power system stability IEEE/CIGRE joint task force on stability terms and definitions," *IEEE Transactions on Power Systems*, vol. 19, no. 3, pp. 1387-1401, 2004.

[3] I. Kaffashan and T. Amraee, "Probabilistic undervoltage load shedding using point estimate method," *IET Generation, Transmission & Distribution*, vol. 9, no. 15, pp. 2234-2244, 2015.

[4] C. W. Taylor, *Power System Voltage Stability*, McGrawHill, Inc., 1994.

[5] N. G. Hingorani and L. Gyugyi, *Understanding FACTS: Concepts and Technology of Flexible AC Transmission Systems*, New York: IEEE Press, 2000.

[6] A. Sode-Yome, N. Mithulananthan, and K. Y. Lee, "A comprehensive comparison of FACTS devices for enhancing static voltage stability," in *Proc. IEEE Power Engineering Society General Meeting*, 2007.

[7] J. W. Simpson-Porco and F. Bullo, "Distributed monitoring of voltage collapse sensitivity indices," *IEEE Transactions on Smart Grid*, vol. 7, no. 4, pp. 1979-1988, 2016.

[8] P. Kessel and H. Glavitsch, "Estimating the voltage stability of a power system," *IEEE Transactions on Power Delivery*, vol. 1, July 1986.

[9] B. Gao, G. K. Morison, and P. Kundur, "Voltage stability evaluation using modal analysis," *IEEE Transactions on Power Systems*, vol. 7, November 1992.

[10] R. Tiwari, K. R. Niazi, and V. Gupta, "Line collapse proximity index for prediction of voltage collapse in power systems," *International Journal of Electrical Power & Energy Systems*, vol. 41, no. 1, pp. 105-111, 2012.

[11] M. S. Kumari, G. Priyanka, and M. Sydulu, "Modelling of thyristor controlled series compensator in fast decoupled load flow solution for power flow control," in *Proc. IEEE International Power and Energy Conference*, 2006.

[12] S. Ratra, P. Singh, and R. Tiwari, "A novel approach for modelling of TCSC in load flow solution using NR and automatic differentiation," in *Proc. Annual IEEE India Conference*, 2015, pp. 1-6.

[13] C. R. Fuerte-Esquivel, E. Acha, and H. Ambriz-Perez, "A thyristor controlled series compensator model for the power flow solution of practical power networks," *IEEE Transactions on Power Systems*, vol. 15, no. 1, pp. 58-64, 2000.

[14] S. Sreejith, S. P. Simon, and M. P. Selvan, "Power flow analysis incorporating firing angle model based TCSC," in *Proc. IEEE International Conference on Industrial and Information Systems*, 2010.

[15] L. Wang, C. S. Lam, and M. C. Wong, "A hybrid-STATCOM with wide compensation range and low DC-link voltage," *IEEE Transactions on Industrial Electronics*, vol. 63, no. 6, pp. 3333-3343, 2016.

[16] S. Meikandasivam, R. K. Nema, and S. K. Jain, "Behavioral study of TCSC device–A MATLAB/Simulink implementation," *Proceedings of World Academy of Science Engineering & Technology*, 2008.

[17] S. B. V. S. P. Sastry and V. V. S. K. Rao, "Application of generalized Taguchi and design of experiment methodology for rebar production at an integrated steel plant," *International Journal of Mechanical, Aerospace, Industrial, Mechatronic and Manufacturing Engineering*, vol. 10, no. 6, pp. 898-906, 2016.

Saurabh Ratra received his B.E. (Hons.) degree from University of Rajasthan, Jaipur, India, and M.Tech degree from Punjab Technical University, Jalandhar, India. He is currently working toward the Ph.D. degree in the Department of Electrical Engineering, Malaviya National Institute of Technology, Jaipur, India.

Pradeep Singh received his Bachelor of Engineering degree (2009) in Electrical Engineering from Maharashi Dayanand University, Rohtak and his Master's degree (2013) from Rajasthan Technical University, Kota in Power System. Now he is working as a research scholar in Malaviya National Institute of Technology, Jaipur, India.

Rajive Tiwari received his B.E. (Hons.) and M.Tech (Hons.) degrees in Electrical Engineering from University of Rajasthan, Jaipur, India in 1994 & 1997 respectively, and the Ph.D. degree in Electrical Engineering from the Malaviya National Institute of Technology, Jaipur, India in 2013. Presently, he is serving as Associate Professor in the Department of Electrical Engineering, Malaviya National Institute of Technology, Jaipur, India.